Synthesis and Structure of an Extended Cluster Lead(II) Carboxylate, $[Pb\{(CO)_9Co_3(\mu_3\text{-}CCO_2)\}_2]_n$. Role of Core Metals in Cluster-Derived Hydrogenation Catalysts

Xinjian Lei,[†] Maoyu Shang,[†] Atul Patil,[‡] Eduardo E. Wolf,*[,‡] and Thomas P. Fehlner*[,†]

Department of Chemistry and Biochemistry and Department of Chemical Engineering, University of Notre Dame, Notre Dame, Indiana 46556

Received November 22, 1995[⊗]

The reaction of lead acetate with $(CO)_9Co_3(\mu_3\text{-}CCOOH)$ leads to the formation of $[Pb\{(CO)_9Co_3(\mu_3\text{-}CCO_2)\}_2]_n$, **I**, in high yield. The structure of **I** exhibits unusual six-coordinate Pb(II) centers with two asymmetrical chelating cluster carboxylates ($C_{22}Co_6PbO_{22}$; triclinic $P\bar{1}$; $a = 8.119(1)$, $b = 14.346(2)$, $c = 14.660(2)$ Å; $\alpha = 102.18(1)$, $\beta = 99.01(1)$, $\gamma = 97.30(1)°$; $Z = 2$). One oxygen of each cluster carboxylate ligand bridges between adjacent lead atoms such that a chainlike extended structure is found in the solid state without the presence of solvent or water. **I** is converted stepwise on pyrolysis into two metastable forms of solid materials (designated LT and HT), each of which has been characterized spectroscopically. The hydrogenation of 2-butenal as a test reaction shows that the LT catalyst exhibits selectivities similar to previous LT materials derived from other cobalt cluster metal carboxylates and that the HT material is totally inactive. The observed release of the lead core metal under HT activation conditions totally inactivates the catalyst and demonstrates exposure of the core metal in the HT form of these novel catalysts.

Introduction

While the use of organometallic complexes as catalyst precursors is well-known,[1] the use of chemically assembled multiclusters as precursors to solids with metastable porous microstructures constitutes a new approach to the preparation of heterogeneous catalysts. In our work to date, we have used a transition metal cluster as a substituent on a ligand as a general strategy for the synthesis of large cluster arrays. Thus, the cluster carboxylic acid, $(CO)_9Co_3(\mu_3\text{-}CCOOH)$, gives rise to large cluster carboxylate analogs of metal acetates having the cluster geometries schematically shown in Chart 1.[2,3] The thermolysis of these cluster arrays gives rise to high surface area, largely metallic solids that are amorphous to X-ray and electron diffraction in the temperature range of interest.[4] The spectroscopic data have established two metastable forms of these solids. One is formed at lower temperatures (100−180 °C; loss of CO, which is designated LT), and one, at higher temperatures (200−250 °C; loss of CO and/or CO_2, which is designated HT).[5] These materials are active, stable heterogeneous hydrogenation catalysts for 1,3-butadiene with activities and selectivities that depend on the geometry of the cluster array as well as the identity of the core metal.[6] In fact, the use of large molecules as precursors to heterogeneous catalysts permits the systematic variation of the structural and compositional characteristics of the resulting catalysts. This is clearly demonstrated in the application of our method to the difficult problem of the selective hydrogenation of an α,β-unsaturated aldehyde to the unsaturated alcohol.[7] By variation of the catalyst precursor, good yields of the desired kinetic product can be obtained under mild conditions.

Chart 1

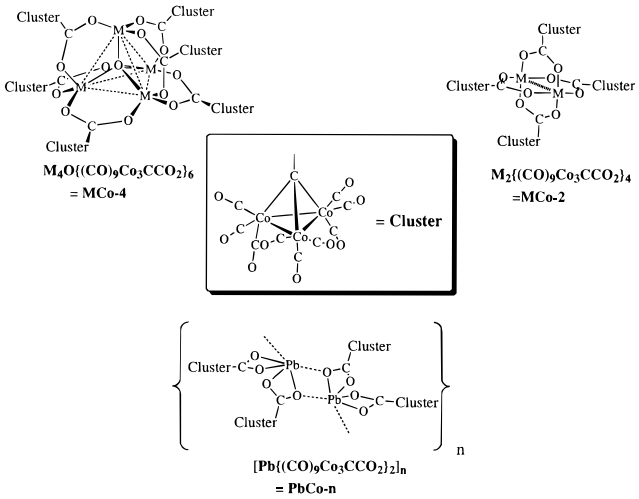

Comparison of both the spectroscopic and catalytic measurements of materials prepared from $Co_4O\{(CO)_9Co_3(\mu_3\text{-}CCO_2)\}_6$ vs $Co_2\{(CO)_9Co_3(\mu_3\text{-}CCO_2)\}_4$ [CoCo-4 vs CoCo-2], $Co_4O\{(CO)_9Co_3(\mu_3\text{-}CCO_2)\}_6$ vs $Zn_4O\{(CO)_9Co_3(\mu_3\text{-}CCO_2)\}_6$ [CoCo-4 vs ZnCo-4], and $Co_2\{(CO)_9Co_3(\mu_3\text{-}CCO_2)\}_4$ vs $Mo_2\{(CO)_9Co_3(\mu_3\text{-}CCO_2)\}_4$ [CoCo-2 vs MoCo-2] demonstrates the role for the cluster assembly geometry, core structure, and the central metal identity in materials properties.[5−7] The use of an assembly of clusters is important as the uncoordinated cluster, $(CO)_9Co_3(\mu_3\text{-}CCOOH)$, alone does not yield materials with the level of activity, the type of selectivity, or the long-term stability of those derived from the cluster arrays. However, it is not clear which

[†] Department of Chemistry and Biochemistry.
[‡] Department of Chemical Engineering.
[⊗] Abstract published in *Advance ACS Abstracts,* May 1, 1996.

(1) *Studies in Surface Science and Catalysis*; Gates, B. C., Guczi, L. H., Knozinger, H., Eds.; Elsevier: New York, 1986; Vol. 29.
(2) Cen, W.; Haller, K. J.; Fehlner, T. P. *Inorg. Chem.* **1993**, *32*, 995.
(3) Cen, W.; Lindenfeld, P.; Fehlner, T. P. *J. Am. Chem. Soc.* **1992**, *114*, 5451.
(4) Cen, W.; Ladna, B.; Fehlner, T. P.; Miller, A. E.; Yue, D. *J. Organomet. Chem.* **1993**, *449*, 19.
(5) Bañares, M. A.; Dauphin, L.; Lei, X.; Cen, W.; Shang, M.; Wolf, E. E.; Fehlner, T. P. *Chem. Mater.* **1995**, *7*, 553.
(6) Bañares, M. A.; Dauphin, L.; Calvo-Perez, V.; Fehlner, T. P.; Wolf, E. E. *J. Catal.* **1995**, *152*, 396.
(7) Bañares, M.; Patil, A. N.; Fehlner, T. P.; Wolf, E. E. *Catal. Lett.* **1995**, *34*, 251.

S0020-1669(95)01498-4 CCC: $12.00

Table 1. Crystallographic Data for $[Pb\{(CO)_9Co_3(\mu_3\text{-}CCO_2)\}_2]_n$

formula	$C_{22}Co_6PbO_{22}$	space group	$P\bar{1}$ (No. 2)
fw	1177.02	Z	2
a, Å	8.119(1)	μ(Mo Kα), cm^{-1}	82.698
b, Å	14.346(2)	λ, Å	0.071 073
c, Å	14.660(4)	transm coeff	0.71−1.0
α, deg	102.18(1)	ρ_{calc}, g cm^{-3}	2.404
β, deg	99.01(1)	T, K	296
γ, deg	97.30(1)	R[a]	0.020
V, Å^3	1625.6(4)	R_w[b]	0.032

[a] $R = \sum(|F_o| - |F_c|)/\sum|F_o|$. [b] $R_w = (\sum w(|F_o| - |F_c|)^2/\sum wF_o^2)^{1/2}$.

aspects of the precursor structure are most important in determining activity and selectivity. In particular, the specific role of the core metals on catalytic activity has not yet been revealed. We thought that the incorporation of a potent catalyst poison as a core metal, e.g., lead, would lead to an inactive catalyst, if the core metal were released during either of our two standard activation procedures. Thus, the objective of the following experiments was to elucidate the role of the core metals rather than seek any improvement in catalytic properties.

Although the catalytic problem drives the synthesis, the structure and properties of the precursor itself are of interest. The effects of a cluster substituent on simple coordination chemistry can be considerably different from those of a simple organic substituent.[8,9] The ability of a cluster to act as either an electron acceptor or donor and the magnitude of its steric bulk[10−14] differ sufficiently from common organic substituents so as to produce differences in coordination mode and geometry. Thus, the comparison of the metal coordination environment and the structural parameters of a cluster lead carboxylate with those of related organic lead carboxylates provided additional impetus to the study.

Experimental Section

Precursor Synthesis. Reactions were performed under nitrogen with standard Schlenk techniques. $Pb(CH_3CO_2)_2 \cdot 3H_2O$ (0.15 g, 0.4 mmol) and $(CO)_9Co_3CCOOH$ (0.39 g, 0.8 mmol) in CH_2Cl_2 were stirred at room temperature for 30 h. Dark-red needles of $[Pb\{(CO)_9Co_3(\mu_3\text{-}CCO_2)\}_2]_n$, **I**, precipitated, and 0.25 g (53% yield) was isolated from the reaction mixture. Anal. Calcd for $C_{22}O_{22}PbCo_6$: C, 22.45; O, 29.90; Pb, 17.60; Co, 30.04. Found: C, 22.58; Pb, 16.60; Co, 28.60. IR (KBr, cm^{-1}): 2108 w, 2047 vs, 2032 sh, 2014 sh, 1465 m, 1365 m, 1332 w, 780 w, 772 m, 701 m, 533 m, 508 m.

Precursor Structure. Crystal data for **I** are summarized in Table 1. Crystals suitable for X-ray diffraction were grown by layering hexane on top of a saturated CH_2Cl_2 solution of **I**. A platelike black crystal with dimensions 0.40 × 0.15 × 0.09 mm was mounted on top of a glass fiber, and data were collected with an Enraf-Nonius CAD4 diffractometer equipped with graphite crystal monochromated Mo Kα radiation (λ = 0.0710 73 Å). The structure was solved by the MULTAN direct method and followed by successive difference Fourier syntheses. Full-matrix least-squares refinements were employed. Full-matrix least-squares refinements with anisotropic thermal parameters for all atoms (460 variables refined) for 4150 reflections converged at R (R_w) = 0.020 (0.032).

Catalyst Preparation. The TGA measurements were carried out under H_2 (100 mL/min, NPT) in a Cahn electrobalance. As shown in Figure 3, the sample was heated in a stepwise fashion from room temperature to 390 K and then to 490 K. BET surface areas were measured with a Quantachrome unit at 77 K with nitrogen as the adsorbate and helium as the carrier gas. Chemical analysis (Galbraith Laboratories, Inc.) of the 490 K material gave 47.88% Co, 30.13% Pb, and 2.29% C. The X-ray photoelectron spectroscopic (XPS) measurements were carried out in a Kratos XSAM-800 spectrometer using a magnesium anode. Samples were prepared *ex situ* and examined as powders mounted on tape. The binding energies are referenced to a C 1s BE of 285.0 eV. The diffuse reflectance infrared spectroscopy (DRIFTS) was carried out in a reaction cell (Harrick Co.) in a FTIR spectrometer (Mattson, Galaxy-2000). Samples were prepared in a KBr matrix and examined in the manner described previously.[5] The XRD measurements were carried out on a Philips 3520 powder diffraction system.

The catalytic activity was measured in a micro-flow reactor which also has been described previously.[5] The catalyst was prepared *in situ* from the precursor at the chosen activation temperature and conditions, and then its activity was measured using the appropriate temperatures, flow condition, and flow compositions. Product analysis was carried out with a Varian 3700 gas chromatograph with a FID detector and a 10% carbowax, 20M chromosorb 80/100 mesh packed column (Alltech).

Table 2. Selected Distances (Å) and Angles (deg) for $[Pb\{(CO)_9Co_3(\mu_3\text{-}CCO_2)\}_2]_n$

Distances			
Pb−Pb′	4.0333(2)	Co22−Co23	2.465(1)
Pb−Pb″	4.1141(2)	Pb−O11	2.550(3)
Co11−Co12	2.4723(8)	Pb−O11′	2.717(3)
Co11−Co13	2.462(1)	Pb−O12	2.378(3)
Co12−Co13	2.4628(9)	Pb−O21	2.522(3)
Co21−Co22	2.4744(9)	Pb−O21″	2.837(3)
Co21−Co23	2.4584(8)	Pb−O22	2.366(4)

Angles			
Pb′−Pb−Pb″	170.43(1)	O11′−Pb−O12	131.4(1)
Co12−Co11−Co13	59.89(3)	O11′−Pb−O21	122.96(9)
Co11−Co12−Co13	59.85(3)	O11′−Pb−O21″	120.13(9)
Co11−Co13−Co12	60.27(3)	O11′−Pb−O22	88.1(1)
Co22−Co21−Co23	59.96(3)	O12−Pb−O21	88.6(1)
Co21−Co22−Co23	59.70(2)	O12−Pb−O21″	99.6(1)
Co21−Co23−Co22	60.34(2)	O12−Pb−O22	83.5(1)
O11−Pb−O11′	80.10(9)	O21−Pb−O21″	79.9(1)
O11−Pb−O12	52.1(1)	O21−Pb−O22	53.2(1)
O11−Pb−O21	130.5(1)	O21″−Pb−O22	132.9(1)
O11−Pb−O21″	129.3(1)	Pb−O11−Pb′	99.9(1)
O11−Pb−O22	89.5(1)	Pb−O21−Pb″	100.1(1)

Results and Discussion

Synthetic and Structural Chemistry. The reaction of lead(II) acetate trihydrate with $[(CO)_9Co_3(\mu_3\text{-}CCOOH)]$ gives a good yield of a dark red crystalline product with a composition $Pb\{(CO)_9Co_3(\mu_3\text{-}CCO_2)\}_2$. No H_2O was found in the product, and the difference in frequency between the symmetric and antisymmetric carboxylate bands (100 cm^{-1}) is more consistent with chelating than with bridging ligands.[15]

The geometric structure of **I** in the solid state can be understood by reference to Figures 1 and 2 and Chart 1, and the selected structural parameters given in Table 2. The primary bonding network is displayed in Figure 1, where it is seen that two cluster carboxylates are chelating a single Pb(II) center. Secondary Pb−O interactions occur between an oxygen atom of each chelating carboxylate and its adjacent Pb(II) thereby creating a chainlike structure and six-coordinate Pb(II) centers (Figure 2). The six Pb−O distances form three sets. For the chelating carboxylate d_{PbO} = 2.372(6) Å for the two oxygens not involved in bridging to the neighboring $Pb\{(CO)_9Co_3(\mu_3\text{-}CCO_2)\}_2$ units and d_{PbO} = 2.536(14) Å for the two that are

(8) Fehlner, T. P.; Calvo-Perez, V.; Cen, W. *J. Electron Spectrosc.* **1993**, *66*, 29.
(9) Cen, W.; Haller, K. J.; Fehlner, T. P. *Organometallics* **1992**, *11*, 3499.
(10) Seyferth, D. *Adv. Organomet. Chem.* **1976**, *14*, 97.
(11) Penfold, B. R.; Robinson, B. H. *Acc. Chem. Res.* **1973**, *6*, 73.
(12) Peake, B. M.; Robinson, B. H.; Simpson, J.; Watson, D. J. *Inorg. Chem.* **1977**, *16*, 405.
(13) Lindsay, P. N.; Peake, B. M.; Robinson, B. H.; Simpson, J. *Organometallics* **1984**, *3*, 413.
(14) Worth, G. H.; Robinson, B. H.; Simpson, J. *J. Organomet. Chem.* **1990**, *387*, 337.
(15) Mehrotra, R. C.; Bohra, R. *Metal Carboxylates*; Academic Press: New York, 1983; p 396.

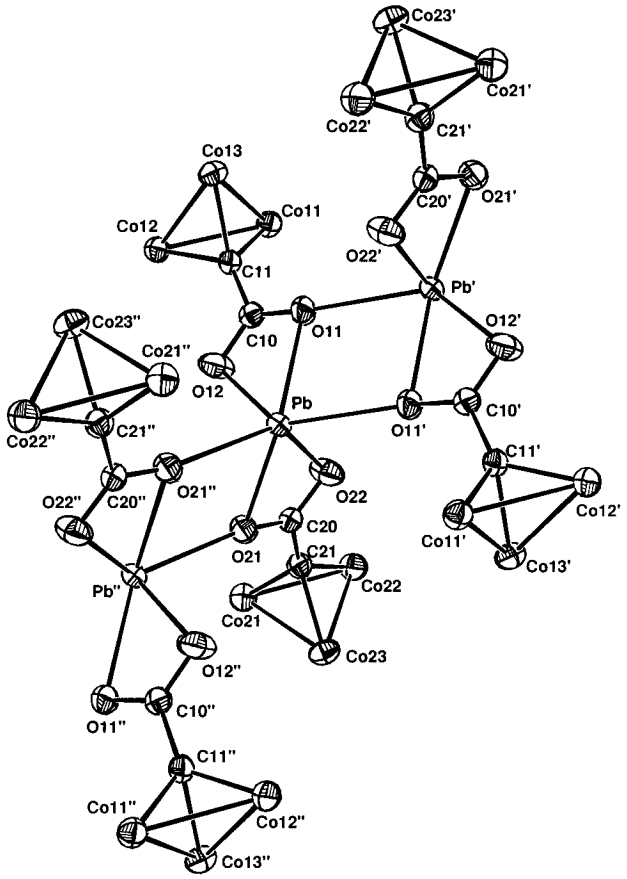

Figure 1. ORTEP diagram showing three Pb{(CO)$_9$Co$_3$(μ_3-CCO$_2$)}$_2$ units in the chainlike structure of **I**. The carbonyl ligands of the tricobalt clusters are omitted for clarity.

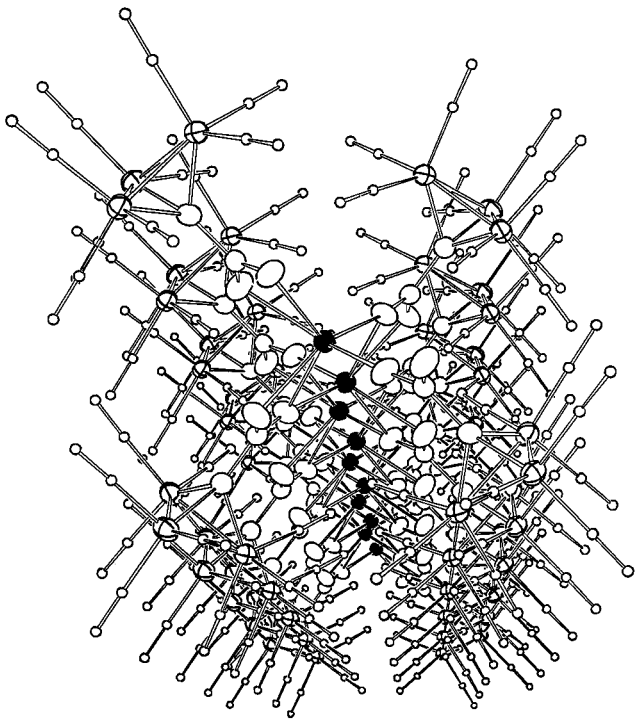

Figure 2. View of the solid-state structure of **I** along the Pb−Pb direction (Pb atoms shaded) showing the columnar cluster array thereby generated.

bridging. For the inter Pb{(CO)$_9$Co$_3$(μ_3-CCO$_2$)}$_2$ unit interactions d_{PbO} = 2.777(60) Å. The angle between the two O−Pb−O planes of the two chelating cluster carboxylates of a given Pb(II) center is 96.67(8)° such that the two tricobalt clusters are adjacent rather than opposed. The tricobalt clusters of the two Pb{(CO)$_9$Co$_3$(μ_3-CCO$_2$)}$_2$ units on either side are disposed 180° with respect to the first leading to the square columnar structure illustrated in Figure 2.

Compound **I** is soluble in THF, and the solution IR shows small differences in the carbonyl region and large differences in the carboxylate region. These observations suggest that the chainlike structure no longer exists in THF. On the other hand, **I** is slightly soluble in CH_2Cl_2 and in this case both the carbonyl (medium) and the carboxylate (weak) regions exhibit the same features as observed in the solid state. Thus, in CH_2Cl_2 the IR measurements suggest that intact fragments of the chainlike structure exist in solution.

Comparison of the structure observed for **I** with those for organic carboxylates reveals significant differences in the substituent properties of the tricobalt cluster compared to an organic substituent. In known Pb(II) carboxylates[16] the coordination number around the Pb(II) center is usually 8 and a variety of stereochemical arrangements of the atoms in the first coordination sphere is found.[17,18] However, coordination numbers of 7,[18] 9,[19] and 10 [20] are also known. Further, the observed solid-state structure is known to depend strongly on the size of the carboxylate substituent. As the substituent becomes progressively bulkier, the structure changes from a polymeric one, to a sheetlike structure, and then to a chain structure.[18] Molecular structures are only observed when a polydentate ancillary ligand is employed.[20] Water (or solvent) plays a special role in some cases either in terms of coordination number or structure. In this case, hydrogen bonding becomes important. Note that the facile formation of lead subacetate also involves the presence of water.[19]

The structure of **I** is most closely related to that of Pb{C_6F_5-COO}$_2$·2CH_3OH.[18] There are two important differences. First, the two organic carboxylato ligands are symmetrically chelating (d_{PbO}= 2.606, 2.591 Å) with Pb−O distances similar to the longer of the two in **I**. The other set of Pb−O distances in **I** is ≈0.2 Å shorter, suggesting stronger Pb−O interactions. Second, in Pb{C_6F_5COO}$_2$·2CH_3OH, two methanol molecules are coordinated to the Pb(II) center (d_{PbO} = 2.709 Å) thereby generating an eight-coordinate Pb(II) center whereas the Pb(II) center of **I** is six coordinate and surrounded only by carboxylate oxygen atoms. Although prepared from the hydrated lead acetate, no water is found in **I**. Apparently the stronger Pb−O coordination, the bulk of the cluster substituent, and the reaction conditions effectively exclude solvent or water from the first coordination sphere of Pb(II). Thus, the electronic effect of the cluster substituent results in stronger coordination and, when combined its steric effect, other ligands are excluded and additional bridging interactions are prevented.

Catalyst Chemistry. The thermogravimetric analysis (TGA) of **I** is shown in Figure 3, and the two-stage weight loss observed is qualitatively characteristic of the behavior of all previous cluster carboxylates studied by us. The temperatures at which the weight losses are observed, Figure 3, are also similar to those observed previously. Consequently, in the same manner as before, the two plateaus can be used to define two metastable forms of the product which are designated LT-PbCo-*n* and HT-

(16) Abel, E. W. In *Comprehensive Inorganic Chemistry*; Pergamon Press: Oxford, U.K., 1973; Vol. 2, p 105.
(17) Williams, D. J.; Maginn, S. J.; Davey, R. J. *Polyhedron* **1994**, *13*, 1683.
(18) Harrison, P. G.; Steel, A. T. *J. Organomet. Chem.* **1982**, *239*, 105.
(19) Bryant, R. G.; Chacko, V. P.; Etter, M. C. *Inorg. Chem.* **1984**, *23*, 3580.
(20) Shin, Y.-G.; Hampden-Smith, M. J.; Kodas, T. T.; Duesler, E. N. *Polyhedron* **1993**, *12*, 1453.

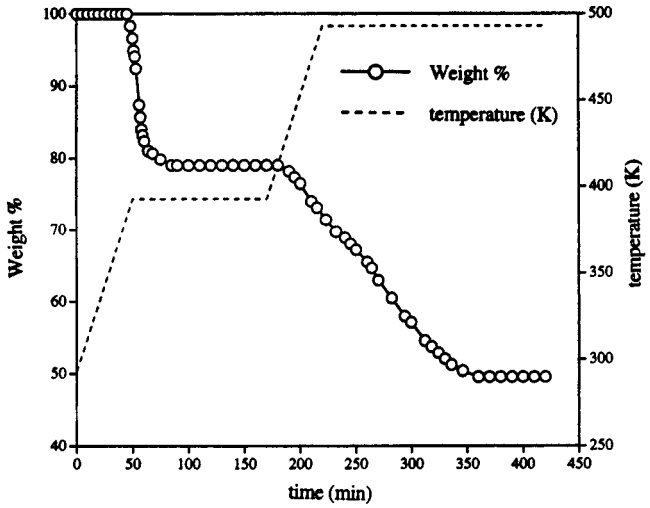

Figure 3. TGA analysis of **I** in H_2. Open circles correspond to sample weight, and the dashed line corresponds to temperature.

PbCo-*n*, respectively. The weight loss at ≈ 400 K is associated with CO loss, but only 9 of the 18 terminal CO ligands are lost in the first decomposition process. The second weight loss is larger, albeit not as sharp timewise. The observed weight loss is 50.5%, and that calculated for the loss of all CO ligands plus two CO_2 molecules is 50.3. This implies a solid composition of Co_6PbC_2 (calcd: Co, 60.46%, Pb, 35.43%, C, 4.11%). The observed analytical results (Co, 47.88%, Pb, 30.13%, C, 2.29%) suggest some oxidation (calcd for $Co_6PbC_2O_6$: Co, 51.94%, Pb, 30.43%, C, 3.53%), which is not surprising on the basis of our previous experience with the bulk analyses of these air-sensitive materials.[4] The oxide formation probably occurs in sample handling due to air oxidation. We conclude that the overall activation of the lead precursor is very similar to that of the other cluster arrays studied previously.

The changes in **I** during pyrolysis were observed in the DRIFTS experiment, and the results are shown in Figure 4 for thermolysis in He and H_2. These experiments are similar to the TGA experiments except that structural aspects of the solid itself are monitored. There is no qualitative difference between the observations in the two reaction atmospheres. In the lowest temperature spectrum, bands characteristic of the tricobalt cluster are seen at ≈2000 cm^{-1} and those characteristic of the chelating carboxylate $-CO_2-$ modes are seen as two sharp bands at 1465 and 1365 cm^{-1}. With increasing temperature, both precursor band types decrease in intensity and broad bands at ≈1900 cm^{-1} in the carbonyl region and 1550 and 1420 cm^{-1} in the carboxylate region grow in.

With one exception, the changes in the carbonyl region mimic those observed previously for other cluster metal carboxylates and demonstrate the total loss of CO ligands. However, it is noteworthy that no intermediate structure with bridging CO bands is observed for **I**. Instead, the changes in the carboxylate region strongly suggest reorganization of the core bonding in the LT region from one in which there are chelating carboxylates to one in which there are bridging carboxylates. Carboxylate core reorganization was suggested for the other precursors, but it is particularly clear for **I** because the splitting of the antisymmetric and symmetric $-CO_2-$ modes for a chelating carboxylate is considerably less than that for bridging carboxylates. Observation of Pb metal in the LT material (XPS below) suggests condensation of the core network with concomitant extrusion of Pb. The LT material is viewed as retaining a carboxylate core (consistent with high surface areas; see below) with cobalt metal and lead exposed to the gas phase (consistent with the XPS and catalytic activity). The DRIFTS spectra show

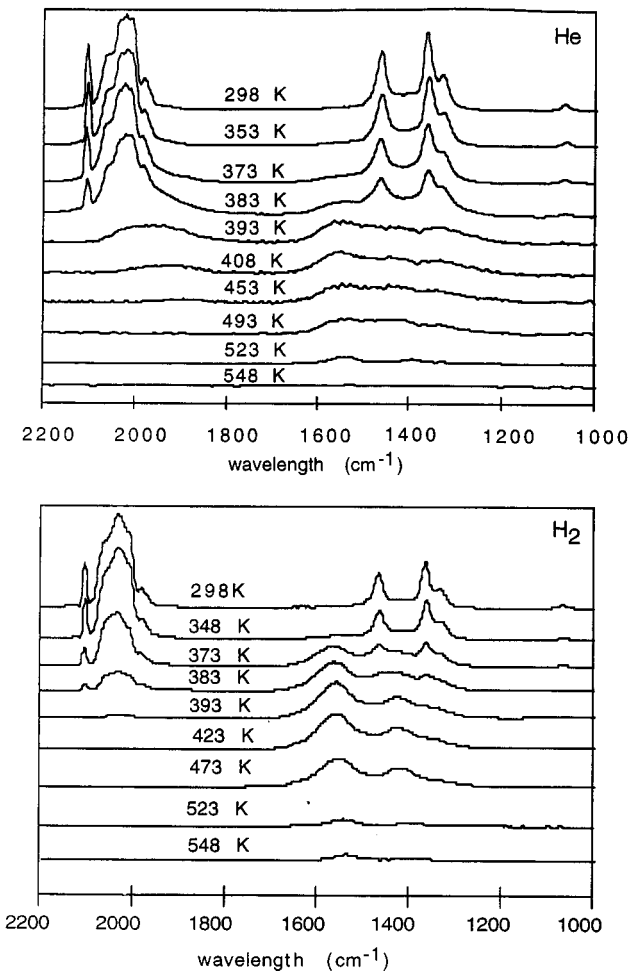

Figure 4. In situ DRIFTS during heating of **I** in He (top) and H_2 (bottom) at a rate of ca. 10 m per spectrum.

total loss of both carbonyl and carboxylate moieties of **I** at the highest temperatures which is consistent with the TGA and bulk analytical measurements.

As expected, the XPS experiments identify the elements C, O, Co, and Pb in the materials. Comparison of data on precursor and catalyst provides information on the bonding states as well as relative abundances of the elements present near the surface. Both LT and HT materials were examined. The C(1s) ionization showed carbon associated with CO ligands of the precursor (BE 288 eV) with a signal intensity that decreased to ≈40% under LT conditions and nearly completely under HT conditions. Signals for carbide carbon (285 eV) and for oxygen (533 eV) were observed under all conditions; however, although the former is expected, the latter is probably introduced during sample handling. The Co(2p) multiplet observed in the precursor is similar to that reported previously.[4] It is observed under LT conditions but was unobservable under HT conditions. Cobalt is present in the catalytic material (see analytical results above) but is not near the surface under HT conditions. XPS is a surface technique that samples 10−20 Å deep with about 10% of the signal from the first atomic layer on the surface.[21] On the other hand, the Pb($4f_{7/2}$) signal (Figure 5) while showing a single Pb(II) signal (BE 140 eV) in the precursor, showed both Pb(0) (BE 138 eV) and Pb(II) signals under LT and HT conditions (in about a 1:1 ratio in the HT case). This is consistent with the presence of some lead(II) (as a carboxylate) and some lead(0) under LT conditions as well as lead(II)

(21) Carlson, T. A. *Photoelectron and Auger Spectroscopy*; Plenum: New York, 1975.

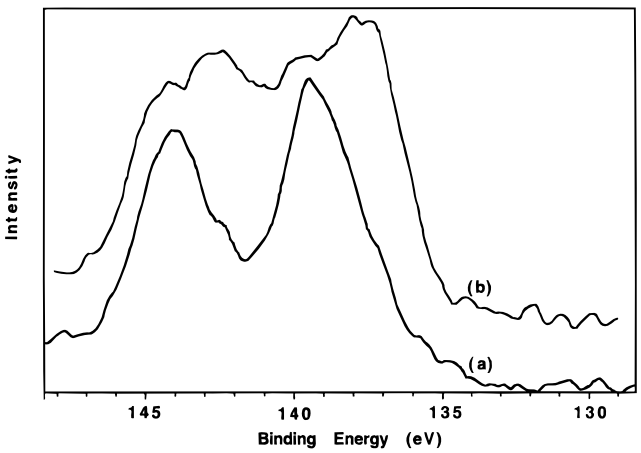

Figure 5. Pb(4f) ionization in the XPS spectra for (a) **I** and (b) the HT-PbCo-*n* material.

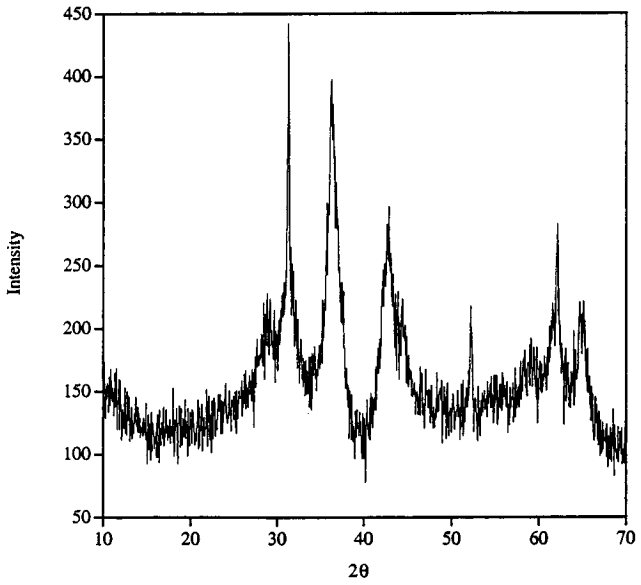

Figure 6. XRD powder diffraction spectrum for HT-PbCo-*n*. The sharp lines arise from Pb, and the broad lines from CoO. Relative particle sizes estimated from line widths are 600 and 100 Å, respectively.

(perhaps as an oxide) and lead(0) under HT conditions. The ratio of Co to Pb, from intensities corrected by standard instrument sensitivities, goes from 7 to ≈1 to ≈0 in going from precursor (calculated Co/Pb = 6) to LT to HT materials, respectively. This shows a substantial build up of Pb in the first 10−20 Å surface layer of the particles of the HT material. Combined with the DRIFTS results this implies that both lead and cobalt are near the surface in the LT catalyst and only lead is near the surface in the HT catalyst.

The XRD results of an HT catalyst sample (Figure 6) are informative (LT catalysts are amorphous). Under these conditions crystallites of lead are observed as well as small crystallites of CoO. No crystalline cobalt metal is observed; however, a small amount would be hidden by the oxide. As noted already, the oxide is thought to originate by air oxidation of the sample during analysis. However, similar examination of ZnCo-4 samples prepared under similar conditions showed only α-Co crystallites and no oxide.[4] The weak intensities of the lines as well as the broad underlying features in the spectrum demonstrates that only a small fraction of the material is crystalline and that a considerable amount of the material remains amorphous in nature. However, these results confirm the formation elemental lead and its mobility.

Table 3. Comparison of Surface Areas for LT- and HT-PbCo-*n* with Those of Related Materials (M^2/g with activation in He)

	LT	HT
PbCo-*n*[a]	49	22
CoCo-4	160	52
CoCo-2	53	65
MoCo-2	60	125
CuCo-2	7	22

[a] Surface area of precursor: 7 M^2/g.

Scheme 1

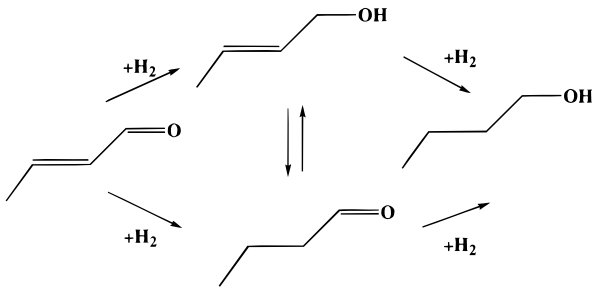

Table 4. Comparsion of Selected Product Distributions (%) for the Catalytic Hydrogenation of 2-Butenal by PbCo-*n* with Those of Related Materials[a]

catalyst	1-butanal	2-butenol	1-butanol	conversion, %
		LT (393 K)		
PbCo-*n*	42	35	19	10
CoCo-4	25	8	64	70
CoCo-2[b]	21	1	78	14
MoCo-2	15	6	76	35
CuCo-2	43	15	38	24
		HT (423 K)		
PbCo-*n*	0	0	0	0
CoCo-4	20	20	60	94
CoCo-2[b]	9	0	86	98
MoCo-2	43	20	30	23
CuCo-2	37	59	0	3

[a] 100% H_2 carrier gas. [b] 25% H_2 in He.

The surface areas are given in Table 3. The area of the LT material is comparable to those observed for the MCo-2 materials as shown in the table whereas the HT material exhibits a decreased surface area with a value on the low side of that observed for other precursors. These data suggest that the rearranged cluster chain of **I** supports significant surface area under LT conditions but that under HT conditions partial breakdown of the porous microstructure occurs. On the basis of Pb−O distances, the inter-Pb{(CO)$_9$Co$_3$(μ_3-CCO$_2$)}$_2$ unit bonding in the extended rodlike structure of **I** is weak and its disruption and rearrangement could well be competitive with Co−CO bond breaking. We have previously observed that the spherical-like particles of Co$_4$O{(CO)$_9$Co$_3$(μ_3-CCO$_2$)}$_6$, which are supported by strong metal−oxygen bonds in the core, give rise to a greater surface area under HT conditions than do M$_2${(CO)$_9$Co$_3$(μ_3-CCO$_2$)}$_4$ with more weakly bonded cores.[5,6]

The final information on the role of the metal core comes from an examination of the hydrogenation of 2-butenal (Scheme 1). The relative number of active sites and their selectivities toward C═C and C═O bond hydrogenation constitute a sensitive probe of the nature of these materials vs the active materials with desirable selectivities studied earlier. Selected results of the catalytic activity of the material prepared from **I** are shown in Table 4 along with results from previous work measured under the similar conditions.

First consider the LT material. Some activity is observed for LT-PbCo-*n* consistent with the exposure of some cobalt

metal to the gas feed. For the same temperature and flow conditions, the conversion is significantly lower for LT-PbCo-*n* than for most of the other LT-MCo materials. As surface areas are comparable, this decrease in activity is attributed to the coverage of many active Co sites with Pb consistent with the spectroscopic measurements described above. Notice that the selectivity for the desired unsaturated alcohol is actually higher than that of any of the other LT materials. However, these selectivities, although reproducible, are sensitive to conditions, particularly in the case of the MCo-2 materials. The selectivity for the saturated aldehyde is about the same as for the earlier catalysts studied whereas that for the saturated alcohol is significantly lower. On the basis of previous results, we believe the activity resides in the exposed cobalt metal in the LT materials and differences in selectivity reside in precursor derived microstructure. We know that the selective formation of the unsaturated alcohol is related to the steric requirements of the unsaturated aldehyde,[7] which implies a sensitivity of the hydrogenation reaction to the geometry of the active site.

The situation is qualitatively different with the HT-PbCo-*n* material. No activity under typical reaction conditions is observed, whereas all previous catalysts, including those derived directly from the cluster ligand $(CO)_9Co_3(\mu_3\text{-}CCOOH)$ and a conventional supported Co catalyst, show some activity. Indeed, it is the HT materials from other precursors that show the optimum selectivity (HT-CoCo-2 with 100% selectivity) and yield (HT-CoCo-4 with 25% yield) for the formation of 2-butenol. The lack of activity for HT-PbCo-*n* is consistent with the spectroscopic results which define the material as one of modest surface area with a single metal, Pb, exposed to the reaction atmosphere. Although there are some differences between this precursor and those studied previously, the similarities are sufficient to establish that the core metal can become of full participant in the catalytic activity in the HT materials. In the case of **I** its role is that of a poison whereas in the case of the active materials it modifies catalyst behavior; i.e., best selectivities are only obtained for the HT materials.

Conclusions. Previous work provided no evidence that the core metals played a direct chemical role in the activities of the catalysts derived from clusters of clusters. Of course the geometrical role in the arrangement of the tricobalt clusters established by the core metals is important. However, it was not possible in the case of the HT-MCo-2 and MCo-4 materials to separate the structural and chemical roles of the core metal atoms. The results from the PbCo-*n* catalysts are unambiguous on this point. The core metal can play a chemical role, and the suicide of the PbCo-*n* catalyst under HT conditions is dramatic evidence of this fact. Thus far, all the MCo materials have displayed reduced activity relative to the CoCo materials; however, several of the MCo materials have desirable selectivities better than those of the CoCo materials. Thus, both the chemical identity of the core metal and the geometry it imposes on the cluster of clusters structure are important in determining the catalytic properties of the derived catalyst.

Acknowledgment. The financial support provided by the National Science Foundation and the Petroleum Research Fund, administered by the American Chemical Society, is gratefully acknowledged. We thank Patrick Pinhero for the XPS measurements and Dr. Xinsheng Liu for the XRD measurements.

Supporting Information Available: Tables of crystal data, atomic positional and displacement parameters, and distances and bond angles for $[Pb\{(CO)_9Co_3(\mu_3\text{-}CCO_2)\}_2]_n$ (7 pages). Ordering information is given on any current masthead page.

IC951498M